



## Executive summary

# Phased array beamforming in wind tunnels



### Problem area

This paper was presented as part of the VKI/EWA Lecture Series on “Experimental Aeroacoustics”, Brussels, 13-17 November 2006.

### Description of work

The practical implementation of phased arrays of microphones in wind tunnels is considered. The contents of this paper are based on array experiences in DNW wind tunnels, both in open and in closed configurations.

### Results and conclusions

This paper consists of three chapters. The first chapter discusses aspects of the experimental set-up,

like microphones and data acquisition, such that a firm basis can be set for measurements. The next chapter is about the limitations of wind tunnel array measurements, like the shear layer in open wind tunnel set-ups, and the boundary layer in closed test sections. The last chapter considers processing (beamforming) techniques which are commonly applied to array measurements in DNW wind tunnels.

### Applicability

The DNW experiences on which this paper is based apply to other wind tunnels as well.

**Report no.**  
NLR-TP-2006-732

**Author(s)**  
P. Sijtsma

**Report classification**  
Unclassified

**Date**  
May 2007

**Knowledge area(s)**  
Aëro-akoestisch en experimenteel aërodynamisch onderzoek

**Descriptor(s)**  
Microphone arrays  
Wind tunnels

This paper was presented as part of the VKI/EWA Lecture Series on “Experimental Aeroacoustics”, Brussels, 13-17 November 2006.





NLR-TP-2006-732

## Phased array beamforming in wind tunnels

P. Sijtsma

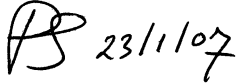
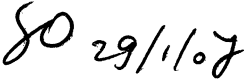
This paper was presented as part of the VKI/EWA Lecture Series on “Experimental Aeroacoustics”, Brussels, 13-17 November 2006.

The contents of this report may be cited on condition that full credit is given to NLR and the author.

This publication has been refereed by the Advisory Committee AEROSPACE VEHICLES.

Customer	European Commission
Contract number	ANE3-CT-2004-502889
Owner	NLR + partner(s)
Division	Aerospace Vehicles
Distribution	Unlimited
Classification of title	Unclassified
	May 2007

Approved by:

Author	Reviewer	Managing department
 23/1/07	 29/1/07	 23/1

## Summary

This paper discusses the practical implementation of phased arrays of microphones in wind tunnels. It consists of a section about the experimental set-up, a section about limitations of wind tunnel array measurements, and a section about processing techniques. The contents of this paper are based on array experiences in DNW wind tunnels, both in open and in closed configurations.

## Contents

<b>1</b>	<b>Introduction</b>	<b>5</b>
<b>2</b>	<b>Experimental set-up</b>	<b>7</b>
2.1	Microphones	7
2.1.1	Free-field or pressure-field	7
2.1.2	Requirements	8
2.2	A/D conversion	8
2.3	Filters	9
2.3.1	High-pass filters	9
2.3.2	Anti-aliasing filters	11
2.4	Data acquisition system	12
<b>3</b>	<b>Limitations</b>	<b>12</b>
3.1	Open configurations	12
3.2	Closed test sections	14
<b>4</b>	<b>Processing Techniques</b>	<b>15</b>
4.1	Diagonal removal	15
4.2	Source power integration	16
	<b>References</b>	<b>19</b>

## Abbreviations

### Symbols

$f$	frequency
$f_{\text{sam}}$	sample frequency

### Abbreviations

AC	Alternating Current
A/D	Analogue-to-Digital
BL	Boundary Layer
CSM	Cross-Spectral Matrix
DC	Direct Current
DR	Diagonal Removal
DNW	German-Dutch Wind Tunnels
FFT	Fast Fourier Transform
LST	Low-speed Wind Tunnel
LLF	Large Low-speed Facility
SNR	Signal/Noise Ratio

## 1 Introduction

Since the mid 1990's, the phased array beamforming technique has rapidly developed into a standard tool for acoustic source location in wind tunnels (Refs. 1-12). In earlier days, acoustic source location was done mainly with elliptic mirrors (Refs. 13-14; Fig. 1), although also investigations were done into the application of phased array techniques (Refs. 15-16). For a long time, the phased array could not outperform the elliptic mirror in spatial resolution, frequency range and signal/noise ratio (SNR). The main reason for this was the limited capacity of data-acquisition systems, so that only a few microphones could be used.



*Fig. 1: Set-up with acoustic mirror in DNW-LLF*

In the 1990's, the phased array technique was boosted by the increasing capacity of computers and data acquisition systems. The application of large numbers of microphones, long acquisition times and high sample frequencies became possible (Ref. 17). Thus, the traditional drawbacks of microphone arrays compared to elliptic mirrors vanished.

The main advantage of phased arrays compared to acoustic mirrors is that only short measurement time is needed, because the process of scanning through possible source locations is done after the measurements by appropriate beamforming software. Measurements with a mirror take a long time, and are hence expensive, since the mirror needs to be adjusted for every possible source location.

The phased array technique is not restricted to acoustics. Before it was applied to acoustic wind tunnel measurements, it was already widely applied in seismology, astronomy and underwater acoustics (sonar). An overview of the beamforming methods that have been developed over the years can be found in Ref. 18. Not every method, however, is applicable to microphone array measurements in wind tunnels, because of the specific difficulties, like a high background noise level, coherence loss, errors in the transfer model, and calibration uncertainties.

This lecture is devoted to the practical implementation of phased arrays in wind tunnels. It consists of a section about the experimental set-up, a section about limitations of wind tunnel array measurements, and a section about processing (beamforming) techniques. The contents of this lecture are based on array experiences in DNW wind tunnels, both in open and in closed configurations. Examples of array measurements in open and closed wind tunnel configurations are shown in Fig. 2 and Fig. 3, respectively.

For a comparable, but more exhaustive, treatise on the implementation of phased arrays in wind tunnels, based on experiences in the USA, the reader is referred to Ref. 19.



*Fig. 2: Out-of-flow array measurements on Airbus A340 model in the open configuration of DNW-LLF (from SILENCE(R)); array shown in red*



*Fig. 3: Wall-array measurements on a Fokker-100 scale model in DNW-LST*

## **2 Experimental set-up**

### **2.1 Microphones**

#### **2.1.1 Free-field or pressure-field**

There are two types of microphones: pressure-field type and free-field type. Usually the free field type is used.

To understand the functioning of a free-field microphone, we need to know that the acoustic pressure at the microphone membrane is not equal to the free-field acoustic pressure, i.e. when the microphone would not be there. The difference between membrane and free-field acoustic pressure is due to the diffraction caused by the microphone, and is dependent on frequency and on angle of incidence. Only at low frequencies the membrane and free-field acoustic pressures are equal.

At zero angle of incidence, the membrane acoustic pressure level is higher than the free-field value. The difference increases with frequency (Ref. 20). A free-field microphone is designed such that its response corrects for this pressure increase at zero incidence, in other words the frequency-dependent response to the free-field acoustic pressures should be as flat as possible. This flat response only holds for zero incidence. At high frequencies, the free-field microphones have a highly direction-dependent response (directivity).

When microphones are built in a wall, which is usually the case in closed wind tunnels, then there is no microphone diffraction. There is only reflection by the wall. In that case pressure-

field type microphones can be used, which are designed to have a flat frequency-response to the membrane pressure itself.

Nevertheless, free-field microphones can be used as well in a wall-mounted array, but then an in-situ calibration (Ref. 19) is required to correct for the absence of the microphone diffraction.

### **2.1.2 Requirements**

#### Frequency range

Since wind tunnel measurements are often done with scale models, the frequencies of interest have to be scaled accordingly (Ref. 21). Therefore, it is necessary to have microphones which are able to measure up to high frequencies, say 50 kHz.

#### Maximum level

The microphones should be able to measure, without distortion, the highest expected unsteady pressure levels. Especially when microphones are mounted flush in a wind tunnel wall, they are subject to high levels (more than 130 dB) of boundary layer (BL) noise.

To suppress BL noise, investigations (Refs. 6, 22) have been done with “recessed arrays”, where the array is mounted in a cavity underneath a perforated plate. However, the applicability of such a device seems to be limited to low frequencies.

#### Minimum level

High-frequency sound usually has low levels. Therefore the electronic noise levels of the microphones should preferably be as low as possible, say lower than 20 dB.

#### Self-noise

When a microphone is mounted flush in a wind tunnel wall, it is subject to BL noise. But additionally, also microphone “self-noise” may be generated. This self-noise is caused by interaction of the boundary layer with microphone geometry details, like a protection grid (Ref. 19). This self-noise depends significantly on the microphone type, and on installation details (Ref. 23). Obviously, a microphone with minimum self-noise has to be selected.

### **2.2 A/D conversion**

The output of a microphone is an alternating current (AC). This AC serves as input for an analogue-to-digital (A/D) converter, which samples the AC at some sample frequency, and stores it in digital format. The number of bits per sample in which the data is stored depends on the type of A/D converter. A typical value is 16 bits, or, equivalently, 2 Bytes per sample. This means that the samples are stored as 2 Bytes integers.

Before the AC enters the A/D converter, it is usually amplified in order to normalise it into a standard range, typically between  $-2V$  and  $+2V$ . If the AC is amplified, then the microphone noise floor is amplified too. Therefore, the use of highly sensitive microphones (say  $> 10$  mV/Pa) is recommended, so that not much amplification is needed.

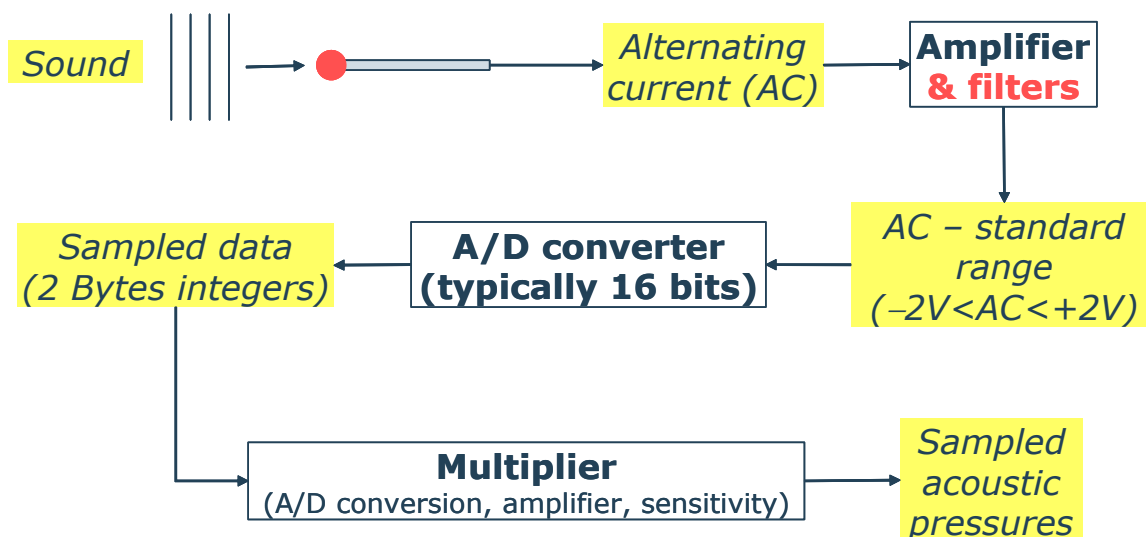


Fig. 4: Data acquisition overview

Finally, to obtain sampled acoustic pressures, the output of the A/D converter needs to be multiplied by some factor, which incorporates the effects of the A/D conversion, the amplifier, and the microphone sensitivity. A graphical overview of the data acquisition chain is plotted in Fig. 4. In the “amplifier” box also “filters” are mentioned. These are discussed in the next section.

## 2.3 Filters

### 2.3.1 High-pass filters

As mentioned in the previous section, in the case of a 16 bits A/D converter, its output is written as 2 Bytes integers. In other words, the output ranges from  $-2^{15}$  to  $+2^{15}$ . The ratio between the highest possible and the lowest possible level is  $2^{15}$ , which is equivalent to 90 dB. In other words, if the amplifier is set such that 2V corresponds to 130 dB, then pressure variations of less than 40 dB will not be represented in the A/D converted output.

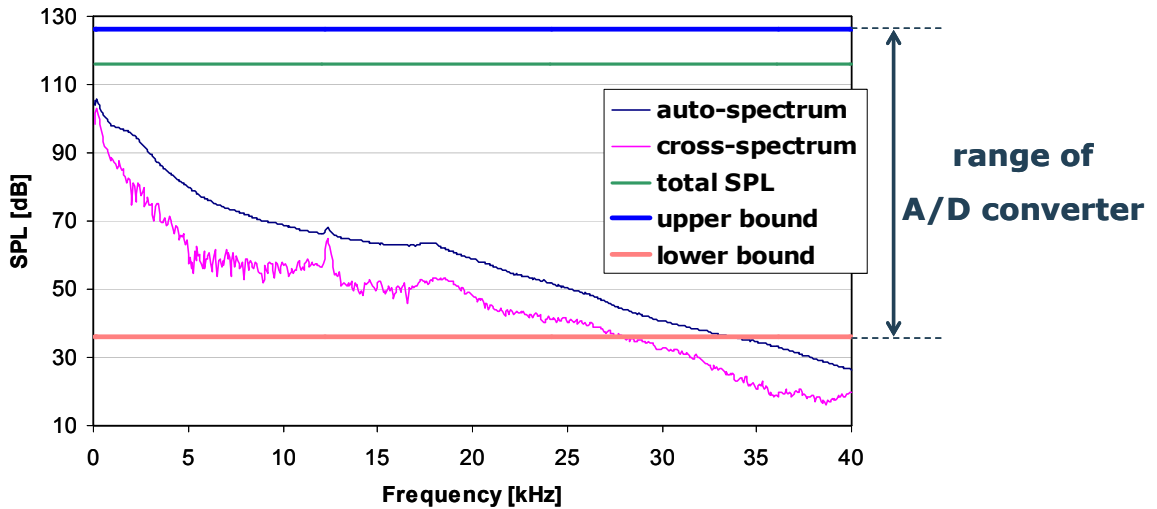


Fig. 5: Typical auto- and cross-spectrum from a wind tunnel wall array measurement

To illustrate this, consider a typical auto-spectrum and a typical cross-spectrum from wall array measurements in DNW-LST (see Fig. 5). The total SPL is 116 dB, which is represented by the green line in the figure. Usually the levels of the peak acoustic pressures are about 5 dB above the total SPL. Including a safety margin, the amplifier will then be set such that the maximum input to the A/D converter (2V) corresponds to approximately 126 dB (blue line). Then, levels lower than 36 dB (below the red line) will not be represented. In the example of Fig. 5 this means that the cross-spectral levels (which contain the most interesting information) at frequencies above 27 kHz are not represented.

A way to extend the represented range of frequencies, using the same 16 bits A/D converter, is the usage of a “high-pass” filter. Such a filter attenuates the AC at frequencies below a certain “cut-off” frequency, and leaves higher frequencies unaltered. The cut-off frequency is defined as the frequency where the attenuation is 3 dB.

In Fig. 6, a high-pass filter is applied to the spectra of Fig. 5. It is a “second order” high-pass filter with a cut-off frequency of 6 kHz. Comparing both figures, it is shown that the high-level, low-frequency part of the spectra is filtered off. Consequently, the total SPL has become much lower: 101 dB. Now the dynamic range of the sampled data is from 21 to 111 dB. As a result, the cross-spectral results are now represented up to 35 kHz.

The true levels can be obtained from Fig. 6 by a simple, frequency-dependent level-correction. This is, in fact, how Fig. 5 was obtained.

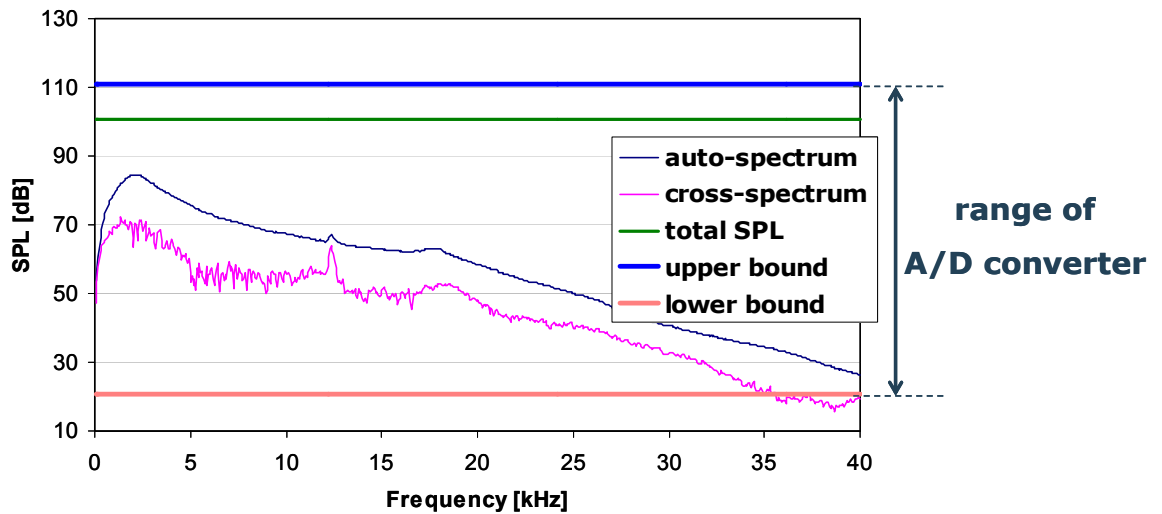


Fig. 6: Filtered auto- and cross-spectrum from a wind tunnel wall array measurement

### 2.3.2 Anti-aliasing filters

If unsteady data is sampled, and then the distinction between frequencies  $f$  and frequencies  $f_{\text{sam}} - f$  is lost ( $f_{\text{sam}}$  is the sample frequency). This phenomenon is called “aliasing” (Ref. 24). An illustration is shown in Fig. 7, where  $f = (1/3)f_{\text{sam}}$  and  $f = (2/3)f_{\text{sam}}$  give identical sampled values.

To avoid this mixing of frequencies, the AC usually passes through a so called anti-aliasing filter before entering the A/D converter. This is a low-pass filter that filters off the frequencies above  $f = (1/2)f_{\text{sam}}$ . The spectra are presented up to  $f = (1/2)f_{\text{sam}}$ , which is called the “Nyquist frequency” or “folding frequency” (Ref. 24).

In contrast with the high-pass filter of Section 2.3.1, an anti-aliasing filter is usually a “high order” filter. This means that the transition region between unaltered frequencies and frequencies that are completely filtered off is small.

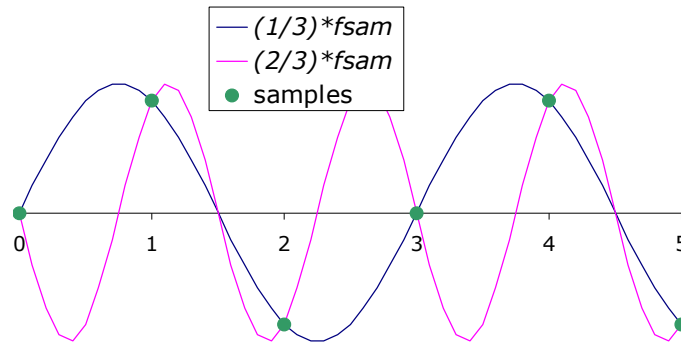


Fig. 7: Illustration of aliasing

## 2.4 Data acquisition system

For a successful acquisition of microphone data the following components are required:

- Signal conditioners (for feeding the microphones with a DC)
- Amplifiers
- Filters
- A/D converters
- A storage device

Together, this is called the “data acquisition system”. In former days, these components were often physically separated. Nowadays, integrated systems can be bought (Ref. 17).

For phased array measurements in wind tunnels, the following properties are required:

- Many channels with synchronous sampling (typically 100 to 140).
- A sampling rate of at least 140 kHz. Then, the Nyquist frequency is 70 kHz. Taking into account a certain band width for the anti-aliasing filter, sound can be analyzed up to 60 kHz.
- The possibility of long acquisition times (typically up to 10 minutes). Herewith, low SNR measurements can be analyzed.
- Several HP and LP filters included.
- At least 16 bits A/D conversion.

## 3 Limitations

### 3.1 Open configurations

Array measurements in an open wind tunnel configuration, where the array is placed out of the flow, are preferred sometimes to closed test sections. This can be because of the following reasons:

- The surrounding test hall can be made anechoic, as in the DNW-LLF (Fig. 8), thus avoiding reflections that are present in closed test sections.
- Array measurements in an open wind tunnel configuration can be done in parallel with traditional devices such as an elliptic mirror and a far-field microphone array.
- The array can be traversed.

A disadvantage of out-of-flow array measurements in an open wind tunnel is the “loss of coherence” due to sound propagation through the turbulent shear layer (Fig. 9). When sound travels through a turbulent medium, it deforms (Refs. 25-28). When sound from a noise source travels along different paths through a turbulent medium, it will deform differently. As a result, the cross-spectral phases of two microphones will be distorted compared to the non-deformed case.

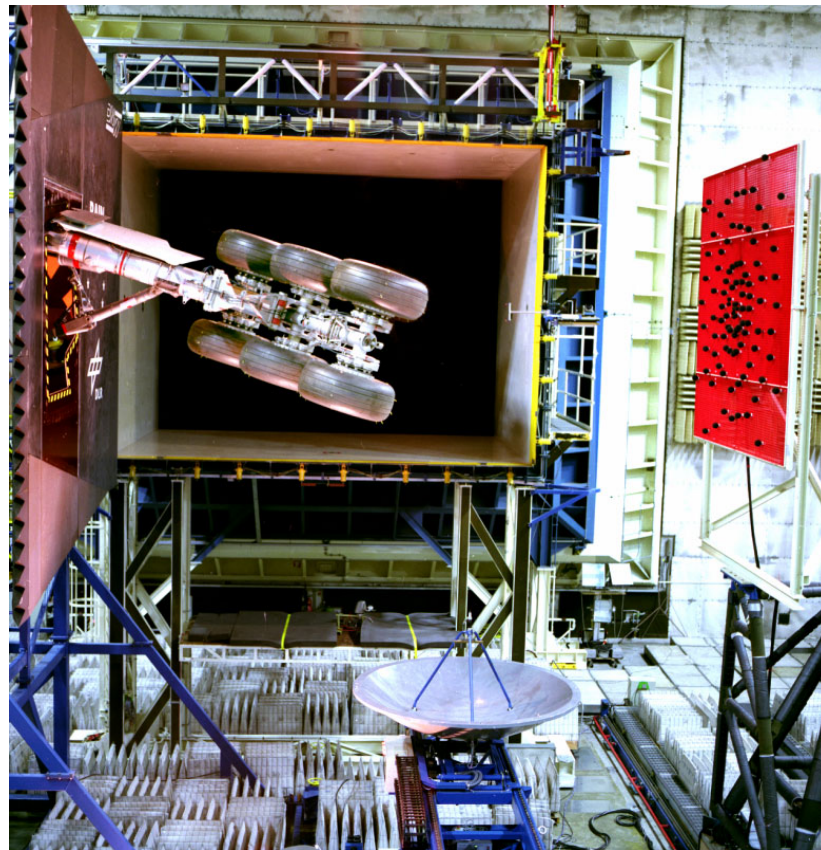


*Fig. 8: Measurements on Airbus A340 full-scale landing gear (RAIN)*

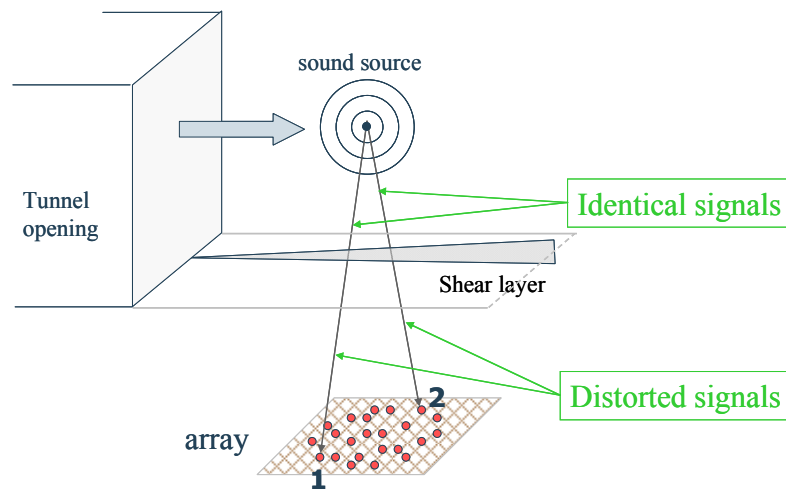


Fig. 9: Loss of coherence due to sound propagation through the shear layer

This phase distortion is different for each FFT-time interval. Therefore, after averaging, the cross-spectral levels are lower than in the non-deformed case. This cross-spectral level reduction is dependent on the turbulence level, the distance between the microphones, the distance between source and microphone and on frequency. At a certain point, the phases are so much distorted that the phase becomes effectively random, and the expected average will be zero. Typically, this phenomenon makes source location in the DNW-LLF open configuration impossible at frequencies higher than 15 kHz.

In Ref. 29 a method to correct for this phase distortion is proposed, which makes use of a well-defined compact sound source, at a sufficiently high level. This method is known as “self-calibration” in radio astronomy, where a “guide star” is used as reference.

### 3.2 Closed test sections

There can be a number of reasons to propagandize array measurements in closed wind tunnel sections:

- There may be some coherence loss in the boundary layer, but this is much less than with the shear layer in an open configuration. Significant data can be obtained up to 50 kHz.
- The distance between array and model can be much shorter than in an open wind tunnel set-up, hence the spatial resolution can be much higher.
- The aerodynamic conditions are better.
- The measurements can be carried out “piggy back”, in parallel to aerodynamic measurements.

There are, however, some restrictions to closed wind tunnel measurements. These will be discussed below.

When a microphone is mounted flush in a wind tunnel wall, it will detect not only acoustic pressures, but also pressure disturbances of hydrodynamic nature due to the turbulent boundary layer. The BL noise levels are often high compared to the sound from a wind tunnel model. Although good beamforming results can be obtained even though the SNR is less than 0 dB, the BL noise levels sets lower bounds to the detectable noise from wind tunnel models.

Another difficulty of closed test sections can be the reflection by the walls. When a sound source gets too close to a wall, the beamforming results become contaminated by the coherent mirror source (Ref. 30). In particular, this can be troublesome when the source has a directivity which is pointing to the wall (like a dipole). However, when the sound source is not directed to the wall, and when there are a few wave lengths of clearance to the wall, this reflection issue does not play a role.

## **4 Processing Techniques**

### **4.1 Diagonal removal**

In wind tunnel array measurements, microphone auto-spectra often have much higher levels than the corresponding cross-spectra. In other words, the main diagonal components of the cross-spectral matrix (CSM) have much higher levels than the off-diagonal components. This happens both in open configurations and in closed test sections, but the causes are different.

In open configurations, cross-spectra are affected by coherence loss, and tend to decrease in level. Since auto-spectra do not contain phase information, their levels are not affected by coherence loss. Hence, auto-spectra tend to dominate the cross-spectral matrix (CSM) when coherence loss becomes significant.

In closed test sections, BL noise is incoherent from one microphone to the other, except when microphones are placed very close to each other in the wind direction, and then only for very low wave numbers (Ref. 31). Therefore, BL noise will appear only in the auto-spectrum, and not in the cross-spectrum. If BL noise has a higher level than sound from a wind tunnel model, which is often the case, then the auto-spectrum dominates.

Because of the diagonal dominance, it is common practice to process wind tunnel microphone array data without the main diagonal of the CSM. Examples of noise source maps obtained without and with diagonal removal (DR) are shown in Fig. 10 and Fig. 11. In Fig. 10 results are shown of measurements on an Airbus A340 model in the open configuration of DNW-LLF (see also Fig. 2), and Fig. 11 shows results from a Fokker-100 model in the DNW-LST, which is a

closed test section wind tunnel (see also Fig. 3). In both cases the improvement in array performance when DR is applied is very large.

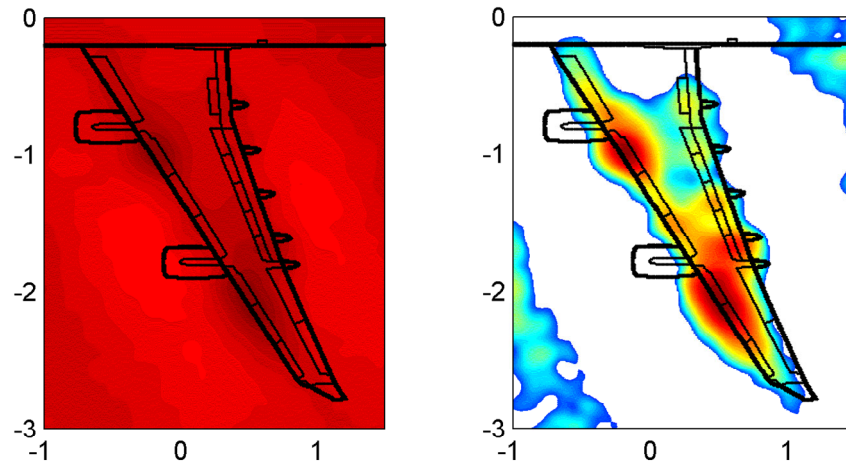


Fig. 10: Noise source maps on an Airbus A340 model in DNW-LLF open configuration, obtained without DR (left) and with DR (right)

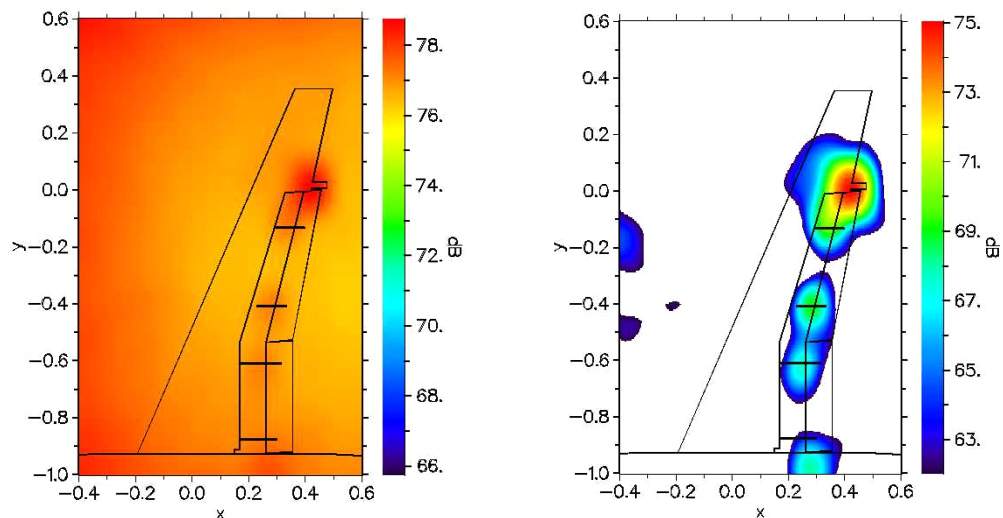


Fig. 11: Noise source maps on a Fokker-100 model in DNW-LST (closed), obtained without DR (left) and with DR (right)

#### 4.2 Source power integration

In a wind tunnel test campaign, often many model configurations are tested, and each configuration at a number of tunnel speeds. Hence, a large number of array measurements needs to be evaluated. Each array measurement delivers source plots for a number of frequency bands, and at each frequency band multiple sources can be present. Thus, a quick assessment of the configuration changes is not easy, because of the large amount of information that is generated.

Obviously, there is a need for further data reduction. This data reduction can be obtained using the technique of “source power integration”, which is outlined below.

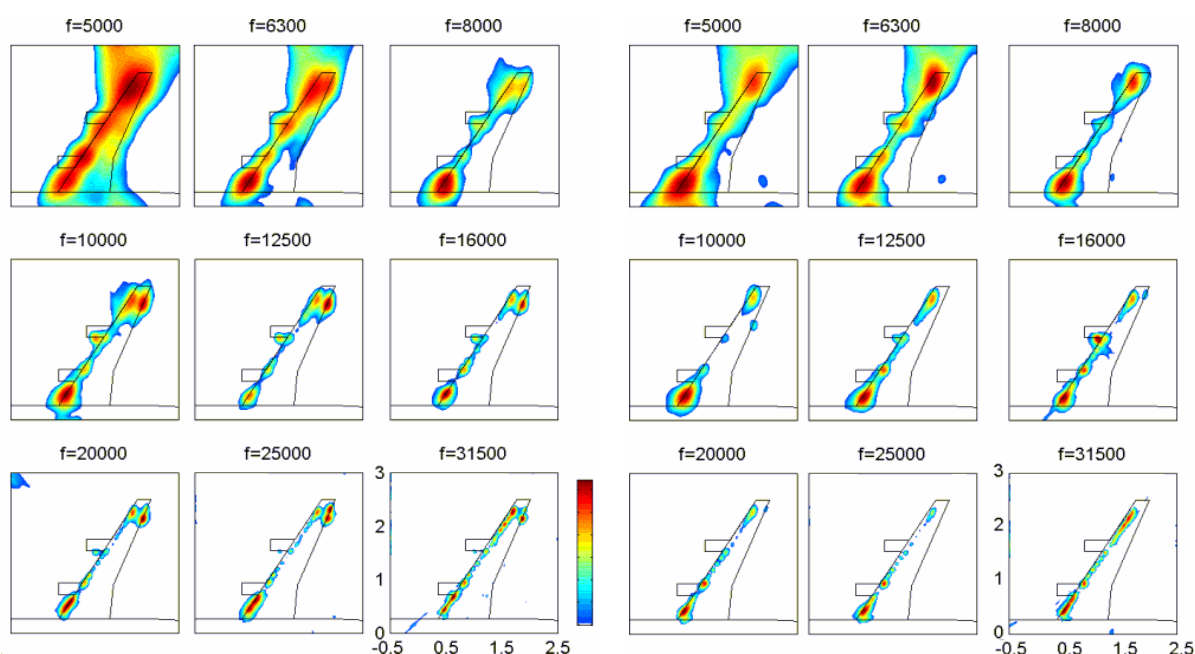


Fig. 12: Array results of two configurations of an Airbus A340 model in closed test section of DNW-LLF; left: configuration A, right: configuration B

To illustrate the need for data reduction, consider two (totally) different configurations of an Airbus 340 model, measured in the  $8 \times 6 \text{ m}^2$  closed test section of DNW-LLF. The source plots of these configurations are shown in Fig. 12. It is very difficult to assess from these plots the relative importance of individual sound sources. Comparison between different configurations and different frequency bands is hampered by the fact the colours do not necessarily correspond. Also overlapping source spots (at lower frequencies) and the non-compactness of some sound sources make an assessment difficult.

Data reduction can be obtained with the “source power integration” technique, described as the “simplified method” in Ref. 32. Herein, a number of areas of interest (integration areas) on the scan plane are allocated (see Fig. 13). On these areas, the source powers obtained by beamforming of all scan points are summed. The result is then divided by the summation of all source powers obtained with a simulated monopole point source (point spread function) in the centre of the integration area. Finally, this ratio is multiplied with the acoustic source power of this point source. The thus obtained integrated source powers give a fairly good estimate of the actual source power radiated from that area.

Integrated results of the three areas are plotted in Fig. 14 (in narrow-band). Now the effects of configuration changes are visible at a glance.

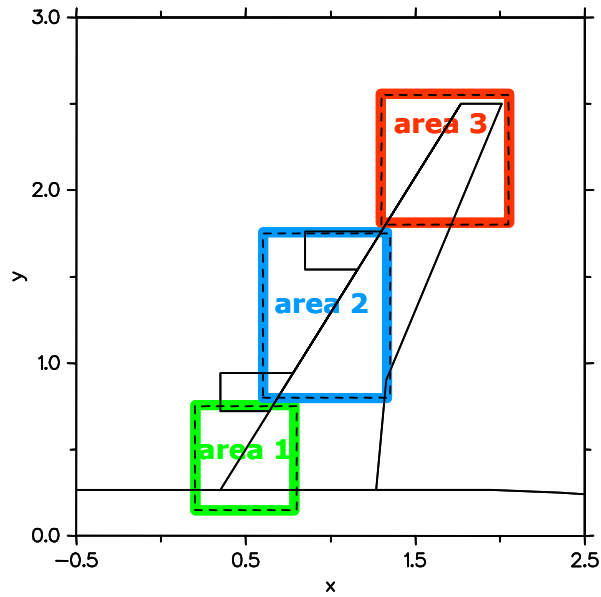


Fig. 13: Integration areas

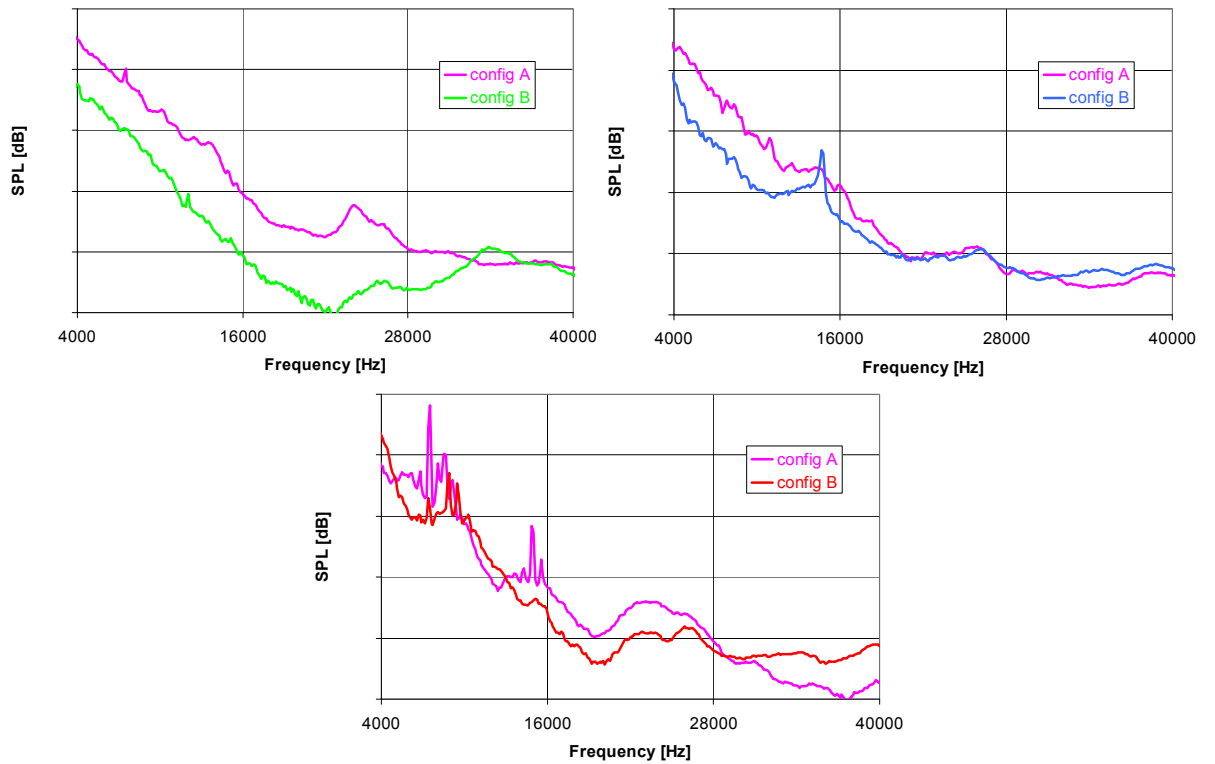


Fig. 14: Integrated results of an Airbus A340 model in closed test section of DNW-LLF; upper left: area 1, upper right: area 2, lower: area 3

## References

1. Hayes, J.A., Horne, W.C., Soderman, P.T., and Bent, P.H., Airframe noise characteristics of a 4.7% scale DC-10 model, AIAA Paper 97-1594, 1997.
2. Meadows, K.R., Brooks, T.F., Humphreys, W.M., Hunter, W.H., and Gerhold, C.H., Aeroacoustic measurements of a wing-flap configuration, AIAA Paper 97-1595, 1997.
3. Dobrzynski, W.D., and Bucholtz, H., Full-scale noise testing on Airbus landing gears in the German-Dutch Wind Tunnel, AIAA Paper 97-1597, 1997.
4. Piet, J.F., and Elias, G., Airframe noise source localization using a microphone array, AIAA Paper 97-1643, 1997.
5. Dassen, A.G.M., Sijtsma, P., Holthusen, H.H., Haaren, E. van, Parchen, R.R., and Looijmans, K.N.H., The noise of a high-speed train pantograph as measured in the German-Dutch Wind Tunnel DNW, Presented at the 2nd International Workshop on the AeroAcoustics of High-Speed Trains, Berlin, 29/30 April 1997, NLR-TP-97409, 1997.
6. Sijtsma, P., and Holthusen, H.H., Source location by phased array measurements in closed wind tunnel test sections, AIAA Paper 99-1814, NLR-TP-99108, 1999.
7. Oerlemans, S., and Sijtsma, P., Effects of wind tunnel side-plates on airframe noise measurements with phased arrays, AIAA Paper 2000-1938, 2000.
8. Dobrzynski, W., Chow, L.C., Guion, P., and Shiells D., A European study on landing gear airframe noise sources, AIAA Paper 2000-1971, 2000.
9. Wal, H.M.M. van der, and Sijtsma, P., Flap noise measurements in a closed wind tunnel with a phased array, AIAA Paper 2001-2170, NLR-TP-2001-632, 2001.
10. Davy, R., and Moens, F., Aeroacoustic behavior of a 1/11 scale Airbus model in the open anechoic wind tunnel CEPRA 19, AIAA Paper 2002-2412, 2002.
11. Stoker, R.W., Guo, Y., Street, C., and Burnside, N., Airframe noise source locations of a 777 aircraft in flight and comparisons with past model scale tests, AIAA Paper 2003-3232, 2003.
12. Oerlemans, S., and Sijtsma, P., Acoustic array measurements of a 1:10.6 Scaled Airbus A340 model, AIAA Paper 2004-2924, 2004.
13. Schlinker, R.H., Airfoil trailing edge noise measurements with a directional microphone, AIAA Paper 77-1269, 1977.
14. Grosche, F.-R., Stiewitt, H., and Binder, B., Acoustic wind-tunnel measurements with a highly directional microphone, *AIAA Journal* Vol. 15., No. 11, pp. 1590-1596, 1977.
15. Fisher, M.J., and Harper Bourne, M., Source location in jet flows, Aeronautical Research Council Report ARC 35/383/N910, 1974.
16. Billingsley, J., and Kinns, R., The acoustic telescope, *Journal of Sound and Vibration*, Vol. 48, No. 4, pp. 485-510, 1976.
17. Holthusen, H.H., and Smit, H., A new data acquisition system for microphone array measurements in wind tunnels, AIAA Paper 2001-2169, 2001.
18. Johnson, D.H., and Dudgeon, D.E., *Array Signal Processing*, Prentice Hall, 1993.
19. Mueller, T.J. (Ed.), *Aeroacoustic Measurements*, Springer, 2002.

20. Brüel, P.V., Sound level meters – the Atlantic divide, Brüel & Kjaer Technical Review No. 4, pp 3-23, 1983.
21. Crighton, D.G., Airframe Noise, in NASA-RP-1258: *Aeroacoustics of Flight Vehicles, Volume 1: Noise Sources*, edited by H.H. Hubbard, pp. 391-447, 1991.
22. Jaeger, S.M., Horne, W.C., and Allen, C.S., Effect of surface treatment on array microphone self-noise, AIAA Paper 2000-1937, 2000.
23. Shin, H., Graham, W., Sijtsma, P., Andreou, C., and Faszer, A., Design and implementation of a phased microphone array in a closed-section wind tunnel, AIAA Paper 2006-2651, 2006.
24. Lynn, P.A., and Fuerst, W., *Introductory Digital Signal Processing with Computer Applications*, Wiley, 1998.
25. Dougherty, R.P., Turbulent decorrelation of aeroacoustic phased arrays: Lessons from atmospheric science and astronomy, AIAA Paper 2003-3200, 2003.
26. Daigle, G.A., Piercy, J.E., and Embleton, T.F.W., Line-of-sight propagation through atmospheric turbulence near the ground, *Journal of the Acoustical Society of America*, Vol. 74, No. 5, 1983, pp. 1505-1513.
27. Tatarski, V.I., The effects of the turbulent atmosphere on wave propagation, Israel Program for Scientific Translations, Jerusalem, 1971.
28. Tatarski, V.I., *Wave Propagation in a Turbulent Medium*, McGraw-Hill, 1961.
29. Koop, L., Ehrenfried, K., and Kröber, S., Investigation of the systematic phase mismatch in microphone-array analysis, AIAA Paper 2005-2962, 2005.
30. Sijtsma, P., and Holthusen, H.H., Corrections for mirror sources in phased array processing techniques, AIAA Paper 2003-3196, 2003.
31. Graham, W.R., A comparison of models for the wavenumber-frequency spectrum of turbulent boundary layer pressures, *Journal of Sound and Vibration*, Vol. 206, No. 4, 1997, pp. 541-565.
32. Brooks, T.F., and Humphreys Jr., W.M., Effect of directional array size on the measurement of airframe noise components, AIAA Paper 99-1958, 1999.